The current issue and full text archive of this journal is available at
www.emeraldinsight.com/0961-5539.htm

A short note on Joule heating in electro-osmotic flows

A consistent non-dimensional scaling

P. Nithiarasu and R.W. Lewis
School of Engineering, Swansea University, Swansea, UK

Received 1 February 2008
Revised 4 June 2008
Accepted 4 June 2008

Abstract

Purpose – The purpose of this paper is to numerically model electro-osmotic flow (EOF), Joule heating and heat transfer in a channel filled with an electrolyte and to introduce a consistent non-dimensional scaling.

Design/methodology/approach – The finite element method along with a fractional step method is employed. Empirical relations for temperature dependent viscosity, electrical and thermal conductivities are also employed. Unstructured meshes are used in the numerical calculations.

Findings – The consistent scaling introduced in the present study is a better and easier way of modelling Joule heating effects in EOF.

Originality/value – The non-dimensional scaling proposed is novel and consistent. The novelty is also introduced in the solution procedure as this is used for the first time to tackle EOF with Joule heating and conjugate heat transfer.

Keywords Flow, Convection, Heat transfer, Finite element analysis, Meshes

Paper type Research paper

Nomenclature

Bi = Biot number
$\mathbf{E}$ = external electric field vector
J = non-dimensional momentum parameter
k = thermal conductivity
k_b = Boltzmann constant (1.381×10^{-23} J/K)
n_0 = bulk concentration of ions (6.022×10^{19} to 6.022×10^{21})
p = pressure (N/m^2)
t = time (s)
u_1 = velocity component in direction 1
z = valence of ion (1)
β = artificial compressibility parameter (m/s)
ϵ_0 = permittivity of the vacuum (8.85×10^{-12} F/m)
μ = dynamic viscosity of the fluid (N m/s^2)
ϕ = external electric potential (V)
ρ_E = power density
ζ = Zeta potential (V)
c_p = specific heat at constant pressure
e = electron charge (1.602×10^{-19} C)
Ju = non-dimensional energy parameter
ka = ratio of electric double layer (EDL) thickness to width of channel
L_∞ = reference length (m)
Pr = Prandtl number
T = temperature (K)
$\mathbf{u}$ = velocity vector (m/s)
$\mathbf{x}$ = coordinate axes (m)
ϵ = dielectric constant (78.5)
λ = electrical conductivity (S/m)
v = dynamic viscosity (μ/ρ) (m^2/s)
ψ = electric potential generated by electro-osmosis (V)
ρ = fluid density (kg/m^3)

This work was partially supported by EPSRC grant D070554/01.

International Journal of Numerical Methods for Heat & Fluid Flow
Vol. 18 No. 7/8, 2008
pp. 919-931

0961-5539
DOI 10.1108/09615530810899024

1. Introduction

Electro-osmotic flow (EOF) is used as pumping, valving, mixing, splitting and delivering mechanisms in "lab-on-chip" devices for biological and chemical analyses and medical diagnoses (Bianchi *et al.*, 2000; Dutta and Beskok, 2001). It is also used in cooling of electronic equipment (Jiang *et al.*, 2002; Zeng *et al.*, 2001). In both the biological and electronic cooling applications, Joule heating can be a major difficulty depending on the electrical conductivity of the electrolyte used and the applied external electric field. In biological applications, the increased use of low cost, but poor heat conductors (Erickson *et al.*, 2003), poses the problem of heat dissipation. In electronic cooling applications, Joule heating increases the temperature of the coolant and imposes an extra burden on the cooling system. Thus, Joule heating and the dissipation of such is one of the major challenges currently faced by heat transfer engineers. The numerical modelling of Joule heating helps to estimate the approximate in-crease in the electrolyte temperature and thus leads to a better device design to dispose the heat generated. In biological (Erickson *et al.*, 2003) and other applications (Arnold, 2007), the presence of conjugate heat transfer is apparent. Thus, a numerical model should include strategies for dealing with the heat conduction in the surrounding solid, in addition to EOF.

A limited number of modelling studies have been reported on Joule heating and different non-dimensional scalings have been adopted in these studies (Zhao and Liao, 2002; Erickson *et al.*, 2003; Tang *et al.*, 2003, 2004b, a; Xuan *et al.*, 2004; Huang and Yang, 2006; Tang *et al.*, 2006; Chein *et al.*, 2006; Tang *et al.*, 2007). Though, the scalings used in these works are correct, some of them may not always be convenient and are not sufficiently general to use. In isothermal EOF calculations, the scales introduced, including the ones by the authors (Arnold *et al.*, 2008a, b; Singh *et al.*, 2008), can be difficult to interpret in the presence of heat transfer. This is due to the fact that the non-dimensional parameters identified are not independent of each other. Some of the reported studies use different scales for EOF potential and the external potential (Erickson *et al.*, 2003) and such inconsistancy can also make the interpretation of the results difficult. Some other studies use non-dimensional parameters that are defined in terms of the applied external potential (Zhao and Liao, 2002). This can also be inconvenient as any change in external potential boundary condition needs to be represented by the non-dimensional parameter. Thus, we propose a non-dimensional scaling scheme that is often adopted in the natural convection and conjugate heat transfer studies (Nithiarasu *et al.*, 1998; Nithiarasu, 2008). This scaling is general and can be extremely useful and does not change with the boundary conditions or other variable parameters.

The numerical approach employed here is of an unstructured mesh form and is based on an implicit-explicit arrangement (Singh *et al.*, 2008). In such an approach, the electric potential equations are solved using an iterative solver and the remaining equations are solved using a fully explicit time stepping algorithm. This combination makes the application of flow boundary conditions easier than for other fully implicit type approaches. At the fluid-solid interface, the mesh is sufficiently refined to approximate the flux and temperature continuity.

2. Mathematical model

An electric field is defined as electric force per unit charge. The strength of such a field is determined from the divergence of the electric field as:

$$\nabla \cdot \lambda \mathbf{E} = 0 \tag{1}$$

where λ is the electrical conductivity and the electric field $\mathbf{E}$ is defined as:

$$\mathbf{E} = -\nabla\phi \tag{2}$$

where ϕ is the electric potential. Thus, the equation governing the external electric potential may be written as:

$$\nabla \cdot (\lambda \nabla \phi) = 0 \tag{3}$$

The electric field generated by uneven distribution of ions near a solid wall may be expressed using a Poisson equation. Since this process is of a generation type, the equation involves a source term that is a function of the charge density, i.e.:

$$\nabla \cdot (\epsilon \nabla \psi) = -\frac{\rho_E}{\epsilon_o} \tag{4}$$

The charge density ρ_E, is related to the ion concentration. Often, a Boltzmann type distribution is assumed for the ion concentration. Assuming a symmetric electrolyte, the charge density may be written as:

$$\rho_E = -2n_0 ze \ \sinh\left(\frac{ze\psi}{k_b T}\right) \tag{5}$$

Thus, the Poisson-Boltzmann equation governing the electric potential may be written as:

$$\nabla \cdot (\epsilon \nabla \psi) = \frac{2n_0 ze}{\epsilon_o} \ \sinh\left(\frac{ze\psi}{k_b T}\right) \tag{6}$$

The artificial compressibility form of the modified Navier-Stokes equations written in a non-conservation form may be written as follows:

Continuity equation:

$$\frac{1}{\beta^2}\frac{\partial p}{\partial t} + \rho \nabla \cdot \mathbf{u} = 0 \tag{7}$$

Momentum equation:

$$\rho\left(\frac{\partial \mathbf{u}}{\partial t} + \mathbf{u} \cdot \nabla \mathbf{u}\right) = -\nabla p + \nabla \cdot \tau - \rho_E \mathbf{E} \tag{8}$$

where:

$$\tau = \mu(\nabla \mathbf{u} + \nabla \mathbf{u}^{\mathrm{T}}) \tag{9}$$

and the energy equation is:

$$\rho c_p\left(\frac{\partial T}{\partial t} + \mathbf{u} \cdot \nabla T\right) = \nabla \cdot (k \nabla T) + \lambda |\mathbf{E}|^2 \tag{10}$$

where the last term in the above equation represents Joule heating. Equations (1), (6)-(8), and (10) along with appropriate boundary and initial conditions, govern EOF through micro-channels. It is also important to note that the electrolyte properties,

such as electrical conductivity (λ), dielectric constant (ϵ), viscosity (μ) and thermal conductivity (k) can also be a function of temperature.

3. Non-dimensional form

Unlike the previously used scales, the following non-dimensional scales are consistent and general. Since actual flow velocities are not known a priori, calculating a Reynolds number a priori is therefore not possible. Thus, the scales should be selected in such a way as to avoid introducing a Reynolds number into the non-dimensional form. It is also important to have a consistent scale for both the external potential and the potential generated by the clustering of ions close to the walls. Bearing in mind the above points, the following scales are selected to non-dimensionalise the governing equations:

$$\begin{aligned} \phi^* &= \frac{\phi}{\phi_\infty}; \quad \psi^* = \frac{\psi}{\phi_\infty}; \quad \beta^* = \frac{\beta L_\infty}{\alpha_\infty}; \quad \mathbf{u}^* = \frac{\mathbf{u}L}{\alpha_\infty}; \\ t^* &= \frac{t\alpha_\infty}{L_\infty^2}; \quad p^* = \frac{pL^2}{\rho\alpha_\infty^2}; \quad T^* = \frac{T - T_\infty}{T_\infty} \end{aligned} \tag{11}$$

where:

$$\alpha_\infty = \frac{k_\infty}{(\rho c_p)_\infty} \tag{12}$$

and the subscript ∞ indicates a reference quantity. Assuming $\phi_\infty = k_b T_\infty / ze$ and substituting the above scales, we obtain the non-dimensional form of the equations as:

Laplace equation:

$$\nabla \cdot (\lambda^* \nabla \phi^*) = 0 \tag{13}$$

where $\lambda^* = \lambda/\lambda_\infty$.

Poisson-Boltzmann equation:

$$\nabla \cdot (\epsilon^* \nabla \psi^*) = ka^2 \sinh\left(\frac{\psi^*}{T^* + 1}\right) \tag{14}$$

where:

$$\epsilon^* = \frac{\epsilon}{\epsilon_\infty}; \quad ka = \left(\frac{2n_0 z^2 e^2 L_\infty^2}{\epsilon_\infty \epsilon_0 k_b T_\infty}\right)^{1/2} \tag{15}$$

The non-dimensional form of the momentum equation is:

$$\left(\frac{\partial \mathbf{u}^*}{\partial t} + \mathbf{u}^* \cdot \nabla \mathbf{u}^*\right) = -\nabla p^* + Pr \nabla \cdot \tau^* + J \sinh\left(\frac{\psi^*}{T^* + 1}\right) \nabla \phi^* \tag{16}$$

where:

$$\nu^* = \frac{\nu}{\nu_\infty}; \quad J = \frac{2n_0 k_b T_\infty L_\infty^2}{\alpha_\infty^2 \rho}; \quad Pr = \frac{c_p \mu_\infty}{k_\infty}; \quad \tau^* = \nu^* (\nabla \mathbf{u}^* + \nabla \mathbf{u}^{*T}) \tag{17}$$

Finally, the non-dimensional form of the energy equation may be written as:

$$\left(\frac{\partial T^*}{\partial t^*} + \mathbf{u}^* \cdot \nabla T^*\right) = \nabla \cdot (\alpha^* \nabla T^*) + Ju \quad \lambda^* \left|\nabla \phi^*\right|^2 \tag{18}$$

where:

$$\alpha^* = \frac{\alpha}{\alpha_\infty}; \quad Ju = \frac{\lambda_\infty k_b^2 T_\infty}{k_\infty z^2 e^2}; \quad \lambda^* = \frac{\lambda}{\lambda_\infty} \tag{19}$$

In the present work, the electrical conductivity, viscosity and thermal conductivity are assumed to be temperature dependent. The temperature dependent relationships are given as.

The electrical conductivity of the electrolyte:

$$\lambda^*(T) = \frac{\lambda}{\lambda_\infty} = [1 + \gamma^* T - T_\infty] = [1 + \gamma^* T^* T_\infty] \tag{20}$$

where γ^* is the slope ($\gamma^* \approx 0.025$ (Tang *et al.*, 2004b)).

The temperature dependent viscosity for the fluid is given as:

$$\nu^*(T) = \frac{\nu}{\nu_\infty} = \frac{0.00276}{\nu_\infty} \exp\left(\frac{1,713.0}{T}\right) 1.0 \times 10^{-6}. \tag{21}$$

and the temperature dependent thermal conductivity ratio for the fluid is:

$$\alpha^* = \frac{k_f}{k_\infty} = \frac{(0.61 + 0.0012 T_\infty T)}{k_\infty} \tag{22}$$

and for the solid:

$$\alpha^* = \frac{k_s}{k_\infty} = \frac{(1.38 + 0.0013 T_\infty T)}{k_\infty} \tag{23}$$

The reference thermal conductivity k_∞, used in this study is assumed to be the thermal conductivity of the electrolyte at the reference temperature.

The important non-dimensional parameters identified above include the Prandtl number, *Pr,* and the parameters *J*, *Ka* and *Ju*. As seen, these parameters are defined using properties of the fluid and geometry that are known a priori for the electrolyte and the geometry used. Thus, determining these parameters independent of each other is straight forward, unlike many other scales commonly employed in the literature. Table I lists various parameters, reference quantities and their values.

4. Solution procedure

It is clear from the previous section that the independent variable, time, appears in some equations but the equations governing the electric fields are time independent. Thus, we solve the electric field equations using a GMRES solver (Singh *et al.*, 2008). To overcome standard difficulties, a fractional step algorithm involving three steps and the energy equation may be written as (asterisks are dropped from the non-dimensional equations for simplicity):

Parameter	Value
α_∞	$0.146 \times 10^{-6}\,m^2/s$
ϵ_∞	78.5
J	0.1-220 (micro-channel size between 1 and 100 μm)
Ju	$0\text{-}10^{-2}$ (depending on the reference electrical conductivity)
Ka	10-80
K_∞	0.6138 W/mK
λ_∞	0.2 S/m
V_∞	$0.8666 \times 10^{-6}\,m^2/s$
ϕ_{in}; ϕ_{out}	134.4; 0.0 (equal to an electric field of 11.679 kV/m)
Pr	5.877
ζ	-3.7 (corresponding dimensional value is 95 mV)
T_∞	298 K

Table I.
EOF and Joule heating parameters

(1) Intermediate momentum:

$$\left(\frac{\Delta\tilde{\mathbf{u}}}{\Delta t} + \mathbf{u}^n \cdot \nabla \mathbf{u}^n\right) = Pr\nabla \cdot \tau^{n+\theta_1} + J \sinh\left(\frac{\psi}{T+1}\right)^{n+\theta} \nabla\phi^{n+\theta} \tag{24}$$

where $\Delta\tilde{\mathbf{u}} = \tilde{\mathbf{u}} - \mathbf{u}^n$ and $\tilde{\mathbf{u}}$ is an intermediate velocity field.

(2) Pressure calculation:

$$(1-\theta_2)\left(\frac{1}{\beta^2}\right)^n \frac{\Delta p}{\Delta t} - \Delta t \nabla^2 p^{n+\theta_2} = -\nabla \cdot \tilde{\mathbf{u}} \tag{25}$$

(3) Momentum correction:

$$\frac{\mathbf{u}^{n+1} - \tilde{\mathbf{u}}}{\Delta t} = -\Delta p^{n+\theta_2} \tag{26}$$

Energy equation:

$$\left(\frac{\Delta T}{\Delta t} + \mathbf{u}^n \cdot \nabla T^n\right) = \nabla \cdot (\alpha^* \nabla T^{n+\theta_1}) + Ju(\lambda |\nabla\phi|^2)^{n+\theta} \tag{27}$$

In the above equations θ_1 and θ_2 vary between 0 and 1 depending on whether equa-tions are treated explicitly, implicitly or semi-implicitly. All the results given in the present work are generated by assuming $\theta = \theta_1 = \theta_2 = 0$ (Arnold *et al.*, 2008a, b; Nithiarasu, 2003; Nithiarasu *et al.*, 2004, 2007; Nithiarasu, 2005; Zienkiewicz *et al.*, 2005; Mynard and Nithiarasu, 2008).

5. Numerical examples

The problem considered here is shown in Figure 1. This is a conjugate heat transfer problem with convective heat transfer boundary condition at the top surface.

The electrolyte is assumed to flow in the rectangular channel subjected to an external electric field along the channel. The temperature of the electrolyte entering the inlet is assumed to be at 298 K. Owing to the symmetry along the centre of the channel, only half of the geometry is used in the calculations as shown in Figure 1. The total length of the channel is ten times the channel width. The non-dimensional boundary conditions for the electric potentials are $\phi_{\text{inlet}} = 136.4$ and $\phi_{\text{exit}} = 0.0$ and the wall (ζ) of -3.7 has been used as the boundary condition for ψ. The channel wall is assumed to be electrically insulated for the external potential and both the inlet and exit boundaries are assumed to have zero flux conditions for ψ. The non-dimensional velocity components on the solid walls are assumed to be zero and the horizontal velocity gradients at inlet and exit are also assumed to be zero. The cold fluid flowing into the channel is assumed to be at a non-dimensional temperature of zero (reference temperature). Apart from the top surface of the solid, the other two side surfaces of the solid part are assumed to be insulated (hatched sides in Figure 1). The fluid flow exit is also assumed to be insulated. On the top surface, convective boundary conditions are assumed and the convective condition in a non-dimensional form is given as:

$$\frac{\partial T}{\partial n} = BiT \tag{28}$$

where n is the normal direction to the top surface and Bi is the Biot number, given as $hL\infty/k\infty$ with h being the heat transfer coefficient.

Figure 2 shows a part of the unstructured mesh used in the calculations. As seen the mesh is refined close to the fluid-solid interface in order to accurately represent the flow and interface heat transfer. A total of about 15,000 elements are used in the fluid part and about 7,000 elements are used in the solid part.

Two different scenarios are considered here. The first one studied is the channel flow without including the solid part of the domain (i.e. without the hatched portion of the domain in Figure 1). In this case, the top side of the channel wall and the channel inlet temperature are assumed to be constant and equal to the reference temperature. This exercise is to predict the increase in temperature with respect to a change in the parameter, Ju, in the absence of conjugate heat transfer. All other parameters are assumed to be constant ($J = 30$). Figure 3 shows the non-dimensional temperature distribution at different horizontal locations for different values of Ju. As seen, the temperature variation is quite rapid close to the inlet and the profiles are almost

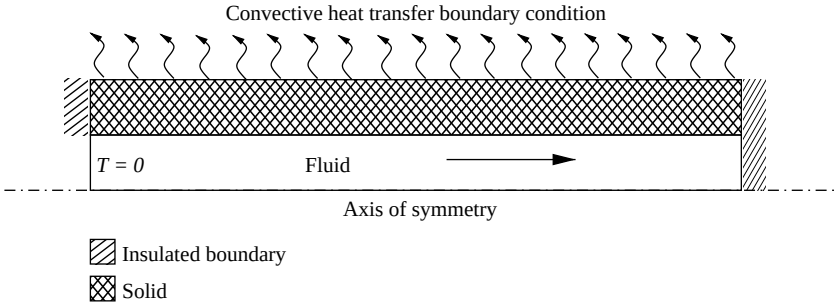

Figure 1.
Domain and boundary conditions

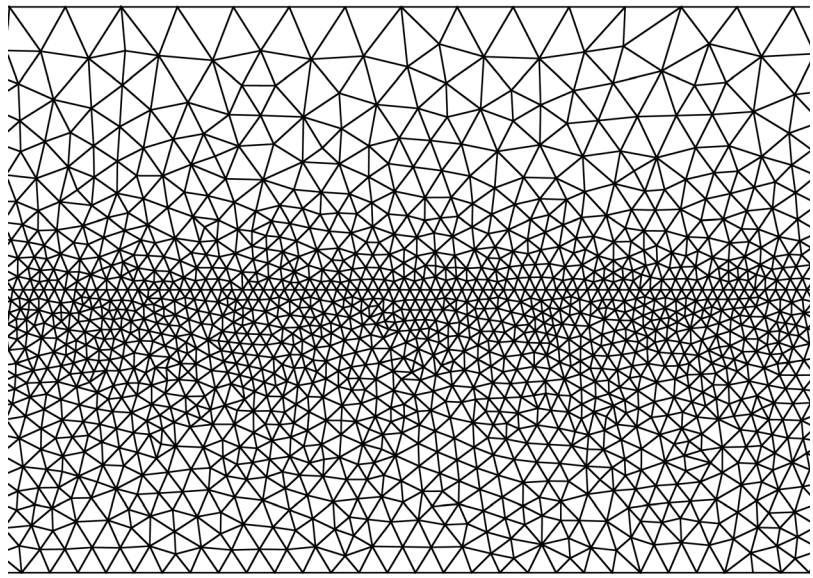

Figure 2.
A short section of the unstructured mesh used

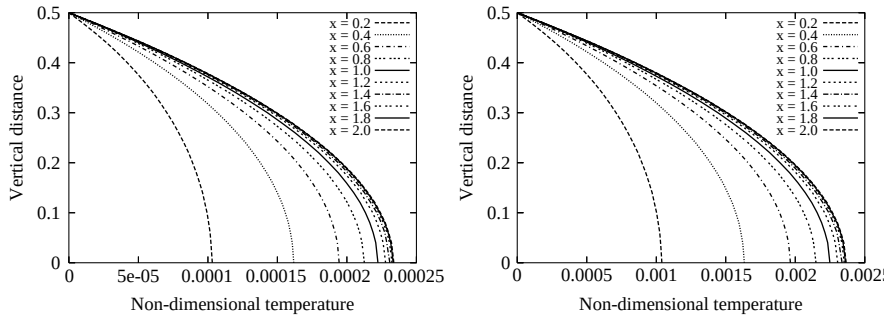

(a) $Ju = 0.00001$

(b) $Ju = 0.0001$

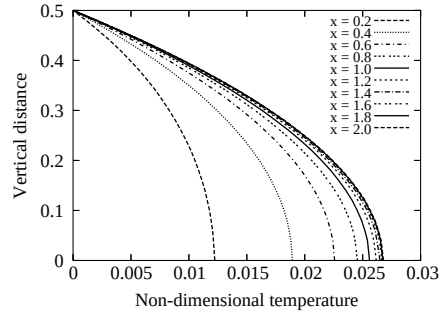

(c) $Ju = 0.001$

Figure 3.
Development of non-dimensional temperature with change in *Ju*

developed at around a non-dimensional distance of 2.0. Since the flow parameters, such as the zeta and external potentials, are fixed then the developing length is almost identical for all three *Ju* values studied. It is also apparent that an order of magnitude increase in the non-dimensional temperature is observed for an order of magnitude increase in the *Ju* value. The maximum dimensional temperatures obtained are: at $Ju = 0.00001$, $T_{max} = 298.06$ K; at $Ju = 0.0001$, $T_{max} = 298.7$ K and at $Ju = 0.001$, $T_{max} = 306.1$ K. Figure 4 shows the non-dimensional temperature distribution along the axis of symmetry. It is again confirmed here that the development length is around 2.0.

The second scenario considered is that of the full conjugate heat transfer problem. The Biot numbers used in the calculations are 10 and 100. Figures 5, 6 and 7 show the results obtained for $Ju = 0.00001$ at $Bi = 10$ and 100. The velocity and external potential clearly indicate the non-linearity introduced. The temperature distribution is smooth without any unusual oscillations close to the interface. The convective boundary condition on the top side is also clearly evident. The differences in temperature distribution at $Bi = 10$ and 100 are clearly shown in Figures 5 and 6.

Figure 7 shows the temperature distribution across the channel and in the solid part of the domain at various locations along the length of the channel. The temperature is almost constant in the fluid part at any section and it varies linearly in the solid portion. It is also clearly evident from Figure 7 that the temperature on the top wall approaches the reference temperature as *Bi* is increased.

6. Conclusions

Modelling of Joule heating in an EOF field is demonstrated using a consistent and standard non-dimensional scale. The scales used are clearly general without the need for prescribing a velocity-based Reynolds number. The examples used include a channel filled with fluid and subjected to conjugate heat transfer. The examples demonstrate clearly that the proposed scales are simple to use and the non-dimensional parameters are easy to determine from the properties of the fluid and from the problems of interest.

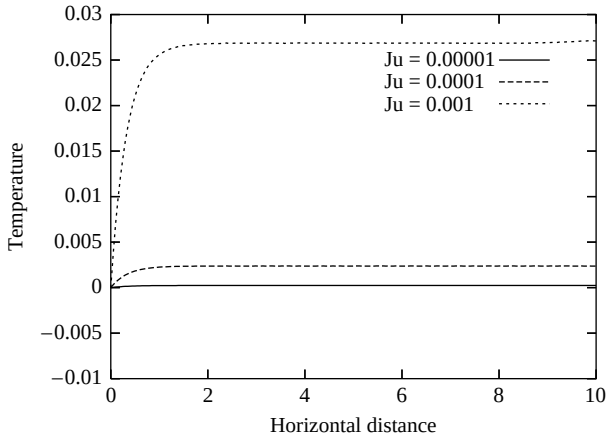

Figure 4.
Temperature distribution along the axis of symmetry

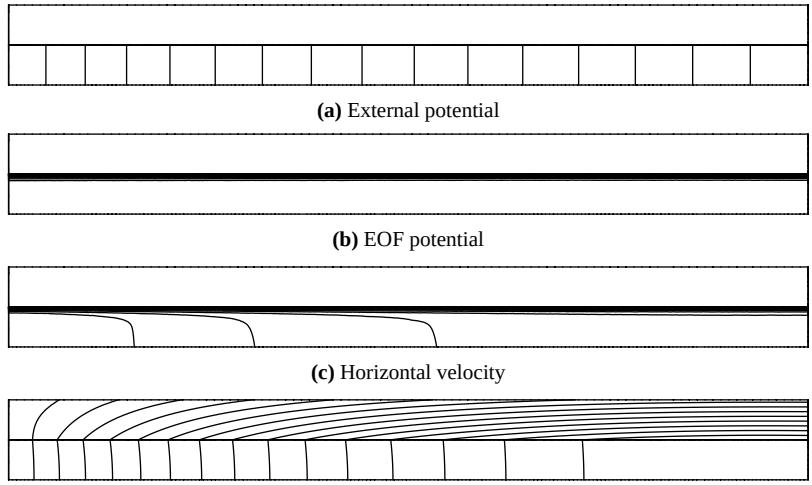

(a) External potential

(b) EOF potential

(c) Horizontal velocity

(d) Temperature

Figure 5.
Conjugate heat transfer in a channel

Notes: Contours of external potential, EOF potential, velocity and temperature Ju = 0.00001, Bi = 10

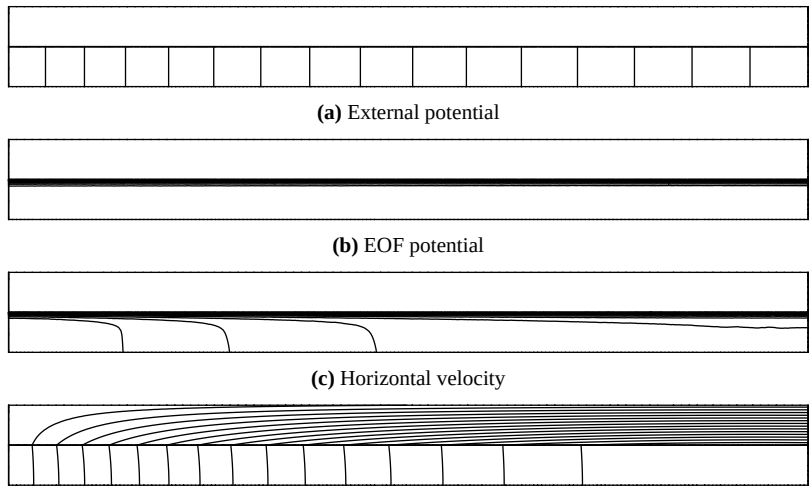

(a) External potential

(b) EOF potential

(c) Horizontal velocity

(d) Temperature

Figure 6.
Conjugate heat transfer in a channel

Notes: Contours of external potential, EOF potential, velocity and temperature Ju = 0.00001, Bi = 100

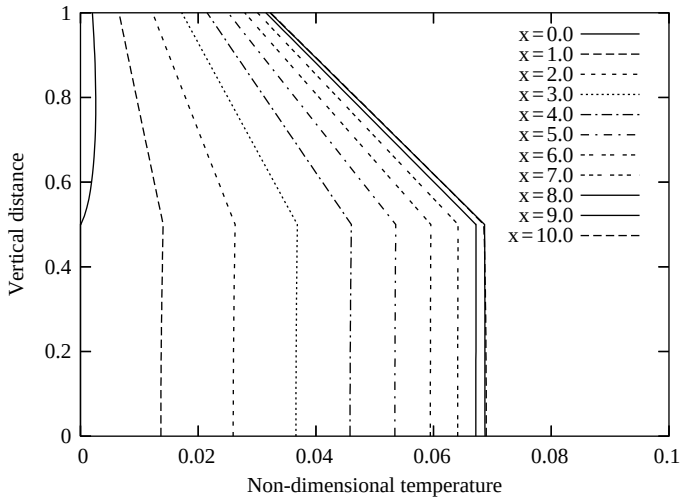

(a) Bi = 10

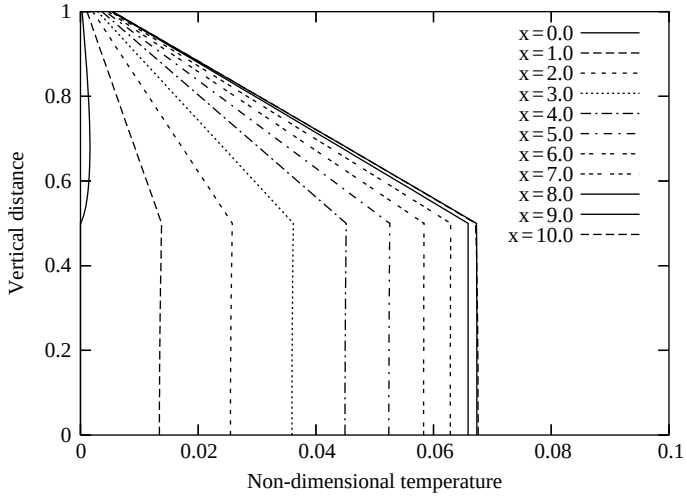

(b) Bi = 100

Notes: Temperature distribution at various horizontal locations Ju = 0.00001

Figure 7.
Conjugate heat transfer in a channel

References

Arnold, A.K. (2007), "Numerical modelling of electro-osmotic flows in micro-channels", PhD thesis, Swansea Univerisity, Swansea.

Arnold, A.K., Nithiarasu, P. and Eng, P.F. (2008a), "Electro-osmotic flow (eof) in micro-channels", *Institution of Mechanical Engineers, Part C, Journal of Mechanical Engineering Science*, Vol. 222, pp. 753-9.

Arnold, A.K., Nithiarasu, P. and Tucker, P. (2008b), "Finite element modelling of electro-osmotic flows using unstructured meshes", *International Journal of Numerical Methods for Heat and Fluid Flow*, Vol. 18, pp. 67-82.

Bianchi, F., Ferrigno, R. and Girault, H.H. (2000), "Finite element simulation of an electro-osmotic driven flow division at a t-junction of microscale dimensions", *Analytical Chemistry*, Vol. 72, pp. 1987-93.

Chein, R., Yang, Y.C. and Liu, Y. (2006), "Estimation of Joule heating effect on temperature and pressure distribution in electrokinetic-driven microchannel flows", *Electrophoresis*, Vol. 27, pp. 640-9.

Dutta, P. and Beskok, A. (2001), "Analytical solution of mixed electroosmotic/pressure driven flows in two dimensional straight channels: finite double layer effects", *Journal of Analytical Chemistry*, Vol. 73, pp. 1979-86.

Erickson, D., Sinton, D. and Li, D. (2003), "Joule heating an heat transfer in poly(dimethylsiloxane) microfluidic systems", *Lab on a Chip*, Vol. 3, pp. 141-9.

Huang, K-D. and Yang, R-J. (2006), "Numerical modelling of the Joule heating effect on electrokinetic flow focusing", *Electrophoresis*, Vol. 27, pp. 1957-66.

Jiang, L., Mikkelsen, J., Koo, J-M., Huber, D., Yao, S., Zhang, L., Zhou, P., Maveety, J.G., Prasher, R., Santiago, J.G., Kenny, T.W. and Goodson, K.E. (2002), "Closed-loop electroosmotic microchannel cooling system for VLSI cirsuits", *IEEE Transactions on Components and Packaging Technologies*, Vol. 25, pp. 347-55.

Mynard, J.P. and Nithiarasu, P. (2008), "A 1D arterial blood flow model incorporating ventricular pressure, aortic valve and regional coronary flow using the locally conservative Galerkin (lcg) method", *Communications in Numerical Methods in Engineering*, Vol. 24, pp. 367-417.

Nithiarasu, P. (2003), "An efficient artificial compressibility (ac) scheme based on the characteristic based split (cbs) method for incompressible flows", *International Journal for Numerical Methods in Engineering*, Vol. 56, pp. 1815-45.

Nithiarasu, P. (2005), "An arbitrary Lagrangian Eulerian (ale) method for free surface flows using the characteristic based split (cbs) scheme", *International Journal for Numerical Methods in Fluids*, Vol. 48, pp. 1415-28.

Nithiarasu, P. (2008), "A unified fractional step method for compressible and incompressible flows, heat transfer and incompressible solid mechanics", *International Journal of Numerical Methods for Heat and Fluid Flow*, Vol. 18, pp. 111-30.

Nithiarasu, P., Liu, C-B. and Massarotti, N. (2007), "Laminar and turbulent flow calculations through a model human upper airway using unstructured meshes", *Communications in Numerical Methods in Engineering*, Vol. 23, pp. 1057-69.

Nithiarasu, P., Seetharamu, K.N. and Sundararajan, T. (1998), "Finite element analysis of transient natural convection in an odd-shapped enclosure", *International Journal of Numerical Methods for Heat and Fluid Flow*, Vol. 8, pp. 199-216.

Nithiarasu, P., Mathur, J.S., Weatherill, N.P. and Morgan, K. (2004), "Three-dimensional incompressible flow calculations using the characteristic based split (cbs) scheme", *International Journal for Numerical Methods in Fluids*, Vol. 44, pp. 1207-29.

Singh, S.P., Nithiarasu, P., Eng, P.F., Lewis, R.W. and Arnold, A.K. (2008), "An implicit- explicit solution method for coupled electro-osmotic flows in three dimensions using un-structured meshes", *International Journal for Numerical Methods in Engineering*, Vol. 73, pp. 1137-52.

Tang, G.Y., Yang, C., Chai, C.J. and Gong, H.Q. (2003), "Modeling of electroosmotic flow and capillary electrophoresis with the Joule heating effect: the Nernst-Planck equation versus the Boltzmann distribution", *Langmuir*, Vol. 19, pp. 10975-84.

Tang, G.Y., Yang, C., Chai, C.K. and Gong, H.Q. (2004a), "Joule heating effect on electroosmotic flow and mass species transport in a microcapillary", *International Journal of Heat and Mass Transfer*, Vol. 47, pp. 215-27.

Tang, G.Y., Yang, C., Chai, C.K. and Gong, H.Q. (2004b), "Numerical analysis of the thermal effect on electroosmotic flow and electrokinetic mass transport in microchannels", *Analytica Chimica Acta*, Vol. 507, pp. 27-37.

Tang, G., Yan, D., Yang, C., Gong, H., Chai, J. and Lam, Y. (2006), "Assessment of Joule heating and its effects on electroosmotic flow and electrophoretic transport of solutes in microfluidic channels", *Electrophoresis*, Vol. 27, pp. 628-39.

Tang, G.Y., Yan, D.G., Yang, C., Gong, H.Q., Chai, J.C. and Lam, Y.C. (2007), "Joule heating and its effect on electrokinetic transport of solutes in rectangular microchannels", *Sensors and Actuators*, Vol. 139, pp. 221-32.

Xuan, X., Sinton, D. and Li, D. (2004), "Thermal end effects on electroosmotic flow in a capillary", *International Journal of Heat and Mass Transfer*, Vol. 47, pp. 3145-57.

Zeng, S., Chen, C-H., Mikkelsen, J.C. Jr and Santiago, J.G. (2001), "Fabrication and characterization of electroosmotic micropumps", *Sensors and Actuators B*, Vol. 79, pp. 107-14.

Zhao, T.S. and Liao, Q. (2002), "Thermal effects on electroosmotic pumping of liquids in microchannels", *Journal of Micromechanics and Microengineering*, Vol. 12 No. 6, pp. 962-70.

Zienkiewicz, O.C., Taylor, R.L. and Nithiarasu, P. (2005), *The Finite Element Method for Fluid Dynamics*, Butterworth-Heinemann, Burlinton, MA.

Corresponding author
P. Nithiarasu can be contacted at: p.nithiarasu@swansea.ac.uk